Amino Acids (2011) 41:173–180
DOI 10.1007/s00726-010-0570-y

ORIGINAL ARTICLE

Redox and metal-regulated oligomeric state for human porphobilinogen synthase activation

N. Sawada · N. Nagahara · F. Arisaka · K. Mitsuoka · M. Minami

Received: 8 January 2010 / Accepted: 15 March 2010 / Published online: 31 March 2010

Abstract The oligomeric state of human porphobilinogen synthase (PBGS) [EC.4.2.1.24] is homooctamer, which consists of conformationally heterogenous subunits in the tertiary structure under air-saturated conditions. When PBGS is activated by reducing agent with zinc ion, a reservoir zinc ion coordinated by Cys^{223} is transferred in the active center to be coordinated by Cys^{122}, Cys^{124}, and Cys^{132} (Sawada et al. in J Biol Inorg Chem 10:199–207, 2005). The latter zinc ion serves as an electrophilic catalysis. In this study, we investigated a conformational change associated with the PBGS activation by reducing agent and zinc ion using analytical ultracentrifugation, negative staining electron microscopy, native PAGE, and enzyme activity staining. The results are in good agreement with our notion that the main component of PBGS is octamer with a few percent of hexamer and that the octamer changes spatial subunit arrangement upon reduction and further addition of zinc ion, accompanying decrease in f/f_0. It is concluded that redox-regulated PBGS activation via cleavage of disulfide bonds among Cys^{122}, Cys^{124}, and Cys^{132} and coordination with zinc ion is closely linked to change in the oligomeric state.

Keywords Analytical ultracentrifugation · Conformational change · Enzyme activity regulation · Negative staining electron microscopy · Porphobilinogen synthase

Introduction

Porphobilinogen synthase (PBGS) [EC.4.2.1.24] catalyzes the condensation of two molecules of 5-aminolevulinic acid (ALA) to produce porphobilinogen in heme biosynthesis pathway. Incorporation of eight zinc ions into the homooctamer human PBGS is regulated by redox potential (Bevan et al. 1980; Cheh and Neilands 1973; Jaffe et al. 1984, 2001; Sawada et al. 2005). A dimer, a minimum structure unit, contains two zinc ions at a maximum; a distal zinc ion which is coordinated by His^{131} and Cys^{223} at an orifice of the active center in one subunit (Erskine et al. 1997), and a proximal zinc ion which is coordinated by Cys^{122}, Cys^{124}, and Cys^{132} near the catalytic sites, Lys^{199} and Lys^{252} in the other subunit (Erskine et al. 2001; Frère et al. 2002; Kervinen et al. 2001; Shoolingin-Jordan et al. 2002). When PBGS was activated by 2-mercaptoethanol (2ME), Cys^{122}, Cys^{124}, and Cys^{132} were simultaneously reduced, and the distal zinc ion was transferred to the proximal zinc ion-binding site, which was catalytically essential (Sawada et al. 2005).

N. Sawada and N. Nagahara contributed equally to the results of this article.
This article is published as part of the Special Issue on Sulfur- and seleno-containing amino acids.

N. Sawada · N. Nagahara (✉) · M. Minami
Department of Environmental Medicine,
Nippon Medical School, 1-1-5 Sendagi Bunkyo-ku,
Tokyo 113-8602, Japan
e-mail: noriyuki@nms.ac.jp

F. Arisaka
Graduate School of Bioscience and Biotechnology,
Tokyo Institute of Technology, 4259-B39, Nagatsuta-cho,
Midori-ku, Yokohama 226-8510, Japan

K. Mitsuoka
Biomedicinal Information Research Center,
National Institute of Advanced Industrial Science
and Technology, 2-41-6, Aomi, Koto-ku,
Tokyo 135-0064, Japan

Thus, the redox-regulated transfer of a zinc ion, and the consequent zinc ion binding triggers the enzymatic activation. For other redox state and/or metal ion-regulated proteins, redox state directly regulates the protein function of 3-mercaptopyruvate sulfurtransferase (report on redox-regulated change of monomer–dimer equilibrium, but no evidence of change in the subunit structure) (Nagahara and Katayama 2005), cystathionine β-synthase (no evidence of redox-induced change in the protein structure) (Pazicni et al. 2005), putidaredoxin (report on redox-induced change of protein surface properties, but no evidence of change in the protein structure) (Sevrioukova 2005), and calbindin (no evidence of redox-induced change in the protein structure) (Cedervall et al. 2005), and NADH:ubiquinone oxidoreductase (estimation of redox-induced change in the protein structure) (Brandt et al. 2003). In some other examples, a metal ion regulates protein function via structural change; e.g. amyloid β-peptide and psoriasin are regulated by zinc ions (Zirah et al. 2006; Li et al. 2005).

As each subunit in the dimeric unit differs in redox state, and consequently differs in zinc ion binding state, the oligomer is microheterogeneous in the tertiary structure although identical in primary structure. In fact, X-ray structure of human wild-type PBGS was only released as PDB code 1E51, and the catalytic cavity of one subunit was obscure probably due to molecular perturbation. The structural heterogeneity made PBGS hard to crystallize and therefore difficult to elucidate the mechanism of PBGS activation.

Human PBGS exists as an equilibrium of functionally distinct quaternary structure assembles, known as "morpheeins", which are a homo-oligomeric protein that can adopt different nonadditive quaternary structure assemblies with different functions (Jaffe 2005).

In the present study, analytical ultracentrifugation (sedimentation velocity and equilibrium analyses), negative staining-electron microscopy, native PAGE, enzyme kinetics, and enzyme activity staining were carried out under physiologically relevant salt conditions. We confirmed that PBGS exists as octamer, as a major component, and hexamer, as a minor component, and provide evidence that the metal and redox-regulated enzymatic activation accompanies change in the quaternary structure to become the fully active form.

Materials and methods

Cloning of human PBGS

Human PBGS was prepared according to our previously reported method (Sawada et al. 2005).

Expression and purification of PBGSs

The constructed vector was transformed into *Escherichia coli* (*E. coli*) BL21 (DE3) which had been previously transformed with a pSTV vector containing GroES and GroEL cDNAs beforehand, which were kindly provided by Dr. Matsumura (Department of Biochemistry and Molecular Biology, Nippon Medical School). Expression and purification of each recombinant PBGS was performed by a modification of our previously reported method (Sawada et al. 2005), which the sample after a gel filtration (Superdex 200, GE Healthcare BioSciences, Buckinghamshire, England) was applied to carboxymethyl cellulose (1.5 × 12.5 cm, CM52, Whatman, Brentford, UK) column equilibrated with 10 mM potassium phosphate buffer, pH 5.8. The enzyme was eluted with a linear gradient of 100 ml of 10–100 mM potassium phosphate buffer, pH 5.8. The enzyme-containing fractions were collected and concentrated with Ultrafree-15 (Millipore, Billerca, USA). After concentration, the buffer of enzyme was changed to 10 mM Tris–HCl buffer, pH 7.4 using Ultrafree-15. The sample was stored at −80°C until use.

Amino acid sequencing of recombinant PBGS was performed using the automated Edman degradation method with a gas phase protein sequencer model 477A (Applied Biosystems Corp., California, USA). To check contaminated proteins other than PBGS, after 3 μg of samples were reduced by 100 mM dithiothreitol and heated at 95°C for 10 min, SDS-PAGE using 12% acrylamide gels was performed (Laemmli 1970). Air-saturated purified PBGS contains six zinc ions per eight subunits (Sawada et al. 2005).

Native PAGE analysis of structural change in the enzymatic activation

To examine a conformational change in the enzymatic activation, 22 μM PBGS (6 zinc ions/octamer) was incubated with 100 μM zinc sulfate (Wako Pure Chemicals, Osaka, Japan) and/or 10 mM commercial (zinc ion-contained) or zinc ion-free 2-mercaptoethanol (2ME, Wako Pure Chemicals) in 100 mM Tris–HCl buffer, pH 7.4 at 37°C for 30 min. PBGS treated with both zinc ions and ME is a reduced PBGS (8 zinc ions/octamer) (Sawada et al. 2005). Zinc ion-free 2ME was prepared by treatment of 1 ml of 100 mM commercial 2ME with 50 mg of Chelex 100 resine (Bio-Rad Laboratories, Inc., Hercules, USA) on ice for 24 h. After incubation, Chelex resine was removed by centrifugation at 18,800*g* for 10 min. For PBGS, the effect of ALA (Sigma-Aldrich Co., St, Louis, USA) on the oligomer size in the enzymatic activation was also examined. Then, 22 μM PBGS was treated with 100 μM zinc sulfate, 10 mM 2ME, and 10 mM ALA in 100 mM Tris–HCl buffer,

pH 7.4 at 37°C for 30 min. After electrophoresis, the gel was stained with Coomassie brilliant blue R250 (Fluka Chemie AG., Buchs, Switzerland) in 30% methanol and 10% acetic acid, and destained.

Effect of oxidation on structural change of PBGSs

To study a conformational change of PBGS by oxidation, 16.53 μM of PBGS was incubated with 200 μM (10-fold molar) and 1 mM (50-fold molar) hydrogen peroxide on ice for 12 h. H_2O (10-fold molar)-oxidized PBGS contains four zinc ions per eight subunits (Sawada et al. 2005). Each sample (8 μg) was applied to a native PAGE (8%). After electrophoresis, the gel was stained with Coomassie Brilliant Blue R250.

Effect of chelation on structural change of PBGSs

To remove the coordinated zinc ions from PBGSs, 16.53 μM PBGS was incubated with 160 μM (10-fold molar) and 800 μM (50-fold molar) EDTA in 100 μl of 100 mM Tris–HCl, pH 7.4 on ice for 16 h. EDTA (10-fold molar)-treated PBGS contains two zinc ions per eight subunits (Sawada et al. 2005). These samples were analyzed by native PAGE, and enzyme activity staining as described below.

Enzyme activity staining

Contaminated zinc ions in 100 mM 2ME were removed by incubation with 1 mM EDTA. After electrophoresis for 8 μg of enzyme using 8% native gel, the gel was soaked in 7 ml of 100 mM bis-Tris propane-HCl, pH 7.0 containing 10 mM commercial (zinc ion-contained), or zinc ion-free 2ME at 37°C for 10 min. Then, 10 mM ALA was added to the mixture and the gel was incubated at 37°C for 20 min. To stop the reaction, the gel was incubated in 3.5 ml of 50% trichloroacetic acid and 100 mM mercury chloride at 25°C for 3 min. The gel was transferred into 10 ml of modified Ehrlich's reagent to color porphobilinogen produced (Mauzerall and Granick 1956), and was incubated at 25°C for 5 min for the activity staining.

Further, to visualize the protein with or without enzymatic activity, after rinsing the gel in double distilled water, the gel was stained with Coomassie Brilliant Blue R250 to check each band.

Electron microscopy

Air-saturated (6 zinc ions/octamer) or reduced PBGS (8 zinc ions/octamer) (0.061 mg/ml) was prepared in 10 mM Tris–HCl, pH 7.4, and reduced PBGS (0.061 mg/ml) was prepared in 10 mM Tris–HCl, pH 7.4 containing 10 mM 2ME and 10 μM $ZnSO_4$. A 2 μl sample was transferred to a glow-discharged carbon-coated copper grid. After 10 s, the drop was blotted with a slice of filter paper. Subsequently, the sample was stained with 2.5 μl of 2% uranyl acetate and air-dried. These stained specimens were examined with a JEM-1230 electron microscope (JEOL, Tokyo, Japan).

Analytical ultracentrifugation of untreated and reduced PBGSs

Air-saturated (6 zinc ions/octamer) or reduced PBGS (8 zinc ions/octamer) (A_{280} = 2.0, 450 μl) was dialyzed against 100 mM Tris–HCl, pH 7.4 (containing 10 μM of $ZnSO_4$, and 10 mM 2ME for reduced sample) at 4°C for 16 h, and each protein was adjusted to the concentrations described below. Both sedimentation velocity and sedimentation equilibrium experiments were performed in an Optima XL-I analytical ultracentrifuge (Beckman-Coulter Inc., Fullerton, USA) in a 4-hole An60Ti or 8-hole An50Ti rotor at 4°C with standard double-sector centerpieces and quartz windows. Concentration profiles of samples were monitored by absorbance at 280 nm. The sedimentation velocity experiments were carried out at A_{280} of 0.85 at a rotor speed of 40,000 rpm. Scans were recorded without intervals between successive scans. In order to examine the effect of ionic strength, PBGS solutions in the presence of 30, 50, 75, and 100 mM potassium phosphate buffer, pH 7.5, containing 100 μM DTT and 10 μM $ZnCl_2$ were prepared by dialysis against these buffers at 4°C for 16 h. Sedimentation velocity data were analyzed with SEDFIT (Schuck 2000). The viscosity and the density of the solvent and partial-specific volume were calculated by SEDNTERP (Philo et al. 1993) and the sedimentation coefficients corrected accordingly.

The sedimentation equilibrium analysis of these samples was performed with A_{280} of 0.2, 0.3, and 0.5, at rotor speeds of 5,000, 6,500, and 8,000 rpm, 4°C. Scans were recorded every 2 h, and the equilibrium of the system was judged by superposition of the last three scans. Global fitting of totally 9 datasets were performed with a software package provided by the manufacturer (Beckman Origin ver. 4.1).

Enzyme assay

PBGS activity was assayed according to previous report (Sawada et al. 2005), the assay mixture contained 10 mM ALA in 0.1 M bis-tris propane buffer, pH 7.0, without 10 mM 2ME and 50 μM zinc sulfate. One unit of enzyme activity was defined as that producing 1 μmol of porphobilinogen per minute.

Protein determination

The protein concentrations were determined with a Coomassie protein assay kit (Pierce Biotechnology, Inc., Rockford, USA) with crystalline bovine serum albumin (Pierce Biotechnology, Inc.) as the standard.

Statistical analysis

All values are expressed as the mean ± standard error (S.E., $n = 3$).

Results

Overexpression and purification of PBGS

SDS-PAGE analysis confirmed that PBGS was purified to homogeneity. The co-expression of PBGS with GroEL and GroES increased the purification yield to about 1.6-fold (0.19 mg/l to 0.31 mg/l).

Native PAGE analysis for conformational change associated with change in the enzymatic activity by redox status

Two bands were observed in native PAGE of PBGS under air-saturated conditions (6 zinc ions/octamer); the upper band will be referred to as the H band and the lower band as the L band, with the H band dominating (Fig. 1a). Both bands were confirmed to be PBGS by using liquid chromatography-mass spectrometer (data not shown). The H and L bands correspond very likely to octamer and hexamer, respectively. Zinc ions alone did not affect these structural changes (Fig. 1a) and enzymatic activation (Sawada et al. 2005). When PBGS is activated with 2ME without zinc ions, both the H and L bands shifted downward with decrease in proportion of the L form (Fig. 1a). These results indicated that the quaternary and/or tertiary structure of PBGS changed accompanying the enzymatic activation. The combined treatment with 2ME and zinc ions increased the specific activity to 8.7-fold that of untreated PBGS (final 8 zinc ions/octamer) (Sawada et al. 2005); and the reduced H band migrated faster, while L band is still present, though faint (Fig. 1a). A substrate, ALA, appears to further reduce the oligomer size and forms a possible reaction intermediate to be a fully active form (Fig. 1a). Activity staining revealed the L forms in untreated PBGS, zinc sulfate-treated PBGS and zinc-free 2ME-treated PBGS are hexamer exhibiting low-enzymatic activity, respectively.

Hydrogen peroxide oxidized PBGS decreasing the specific activity to 1/1.9-fold (Sawada et al. 2005). The migration rate of the H and L bands did not change, but the proportion of the L form increased with increasing concentrations of hydrogen peroxide (Fig. 1b). In this process, 0.7 Zn/subunit was decreased to 0.5 Zn/subunit (Sawada et al. 2005). Enzyme activity staining revealed that the enzyme activity of the H form decreased with increasing

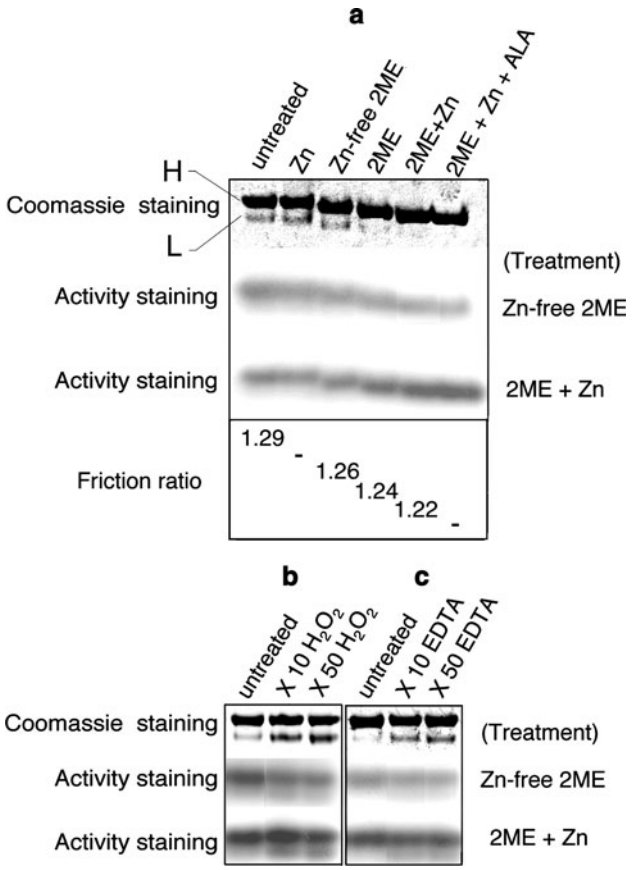

Fig. 1 Native PAGE and enzyme activity staining analyses in the enzymatic activation and inhibition of PBGS. **a** The *top panel* shows the effect of 2ME and/or zinc ions on the oligomer size in the enzymatic activation. After PBGS (6 zinc ions/octamer) was treated with zinc ions, zinc ion-free 2ME (Zn-free 2ME), a commercial 2ME (2ME), 2ME and zinc ions (2ME + Zn), or 2ME, zinc ions, and ALA (2ME + Zn + ALA), native PAGE was performed, and the gel was stained with Coomassie Brilliant Blue R250 (Coomassie staining). H and L bands correspond to octamer and hexamer, respectively. The *middle panel* shows enzyme activity staining (Activity staining) using a staining solution containing zinc ion-free 2ME. The *bottom panel* shows an enzyme activity staining using a staining solution containing 2ME and zinc ions. The *bottom box* shows friction ratios of PBGSs under different conditions, which are determined by analytical ultracentrifugation. Details are described under the text. **b** and **c** The *top panel* shows the effect of hydrogen peroxide (H_2O_2) or EDTA on the oligomer size in the enzymatic inhibition. After PBGS was treated with a 10-fold or 50-fold molar dose of hydrogen peroxide or EDTA, native PAGE was performed, and the gel was stained with Coomassie Brilliant Blue. Each *middle panel* shows enzyme activity staining using a staining solution with zinc ion-free 2ME. Each *bottom panel* shows enzyme activity staining using a staining solution containing 2ME and zinc ions

concentrations of hydrogen peroxide, and the activities of the oxidized H and L forms were increased by 2ME and zinc ions (Fig. 1b), indicating that hydrogen peroxide deprived PBGS of zinc ions, and hence decreased the activity.

Chelation of zinc ions from PBGS with 50-fold molar excess of EDTA decreased the specific activity to 1/1.6-fold that of the control ((6.45 ± 1.07) × 10^{-2} units mg^{-1} to (3.94 ± 1.31) × 10^{-2}), with decrease in the number of zinc ions (0.72 ± 0.05 Zn/subunit to 0.26 ± 0.05) (Cheh and Neilands 1973). The molecular sizes of the H and L bands were unchanged, but the proportion of the L form was increased with increasing concentrations of EDTA (Fig. 1c). Enzyme activity staining revealed that activity of the H form was slightly decreased with increasing concentrations of EDTA, and activity of the chelated PBGS was increased by 2ME and zinc ions (Fig. 1c), confirming that proximal zinc ion binding triggered the enzymatic activation. These results make it evident that redox-regulated enzymatic activation accompanies the binding of proximal zinc ions, which induces a reduction of the Stokes radius of the oligomer as indicated by the decrease in the frictional ratio, f/f_0, and further increases the proportion of the H form.

Negative staining electron microscopic observation for conformational change associated with the enzymatic activation

PBSG both in oxidized and in reduced states were observed by transmission electron microscopy with negative staining. Image of PBGS under air-saturated conditions (Fig. 2a, b, c) shows that four sets of a dimer-unit (an octamer) were major species (Fig. 2b) and three sets of a dimer-unit (a hexamer) were minor ones (Fig. 2c). These images are consistent with deduced top views of an octamer (four sets of a space fill-displayed dimer-unit of human PBGS (PDB entry 1E51)) and a hexamer (three sets of a space fill-displayed dimer-unit) (Fig. 2d). On the other hand, PBGS under reducing conditions appeared homogenous (Fig. 2d). The results suggest that the diminution of the oligomer size is due to a packing of the four sets of the dimer unit.

Analytical ultracentrifugation analysis for conformational change associated with the enzymatic activation

Sedimentation velocity of PBGS under air-saturated conditions (6 zinc ions/octamer) revealed three components with the sedimentation coefficients of 8.24, 10.92, and 14.91 S with relative abundance of 3.6, 88.3, and 8.1%, respectively (Fig. 2e). The distribution function of sedimentation coefficient c (s) was converted into c (M), the distribution function of the molecular mass assuming a common f/f_0, the frictional ratio. The main molecular species has the molecular weight of octamer (275,000), and the small amount of 8.24 S and 14.91 S species correspond to hexamer and possible hexadecimer, respectively. Note that in SEDFIT, the obtained frictional ratio is the weight average of all the species and the s-value of the only major species give a reliable molecular weight. The fact that the global fitting of the concentration gradient of sedimentation equilibrium (Fig. 2f) fits the single species model reasonably well reflects the fact that the gradient mainly consists octamer (88.3%).

When PBGS was activated 8.0-fold that of the control by 2ME and zinc ions (final 8 zinc ions/octamer), a major components with the sedimentation coefficients of 11.4 S (97.0%) and a small amount of 15.9 S (3.0%) were observed (Fig. 2h). The major molecular species has the molecular weight of octamer (262,000), and a minor larger species possibly corresponds to a hexadecimer. The results suggest that the oligomeric state of PBGS under reducing conditions is also mostly octamer with a low concentration of possible hexadecimer, a dimerized octamer. They also demonstrated that the reduced and zinc ion-filled octamer PBGS is more compact than that under air-saturated conditions based on the frictional ratio (f/f_0) of 1.29 for the former and 1.22 for the latter. It is noted that the frictional ratios (f/f_0) of untreated PBGS and zinc ion-free 2ME, 2ME, and zinc ion-added 2ME-treated PBGSs (Fig. 1a) decrease with the degree of enzymatic activation.

The distribution of sedimentation coefficients of wild-type PBSG at a number of ionic strengths, namely 30, 50, 75, and 100 mM of phosphate buffer under reducing conditions is shown in Table 1. A minor peak, a possible hexamer, is more visible in decreasing salt concentrations of the buffer.

It is concluded that the asymmetric shape of octamer appears to approach a more symmetric globule as the enzyme is activated.

Discussion

To determine the oligomeric states of PBGS in solution, analytical ultracentrifugation was carried out, which is most reliable among the methods we used in this study. It is concluded that PBGS (6 or 8 zinc ions/octamer) exists as octamer as a major molecular species with a minor amount of hexamer under physiologically relevant salt conditions and pH. When analytical ultracentrifugation of untreated PBGS (6 zinc ions/octamer) was performed in 30 and 100 mM phosphate buffer, pH 7.5, a possible hexamer was observed and the ratio of octamer to hexamer was 86 to 5.5, and

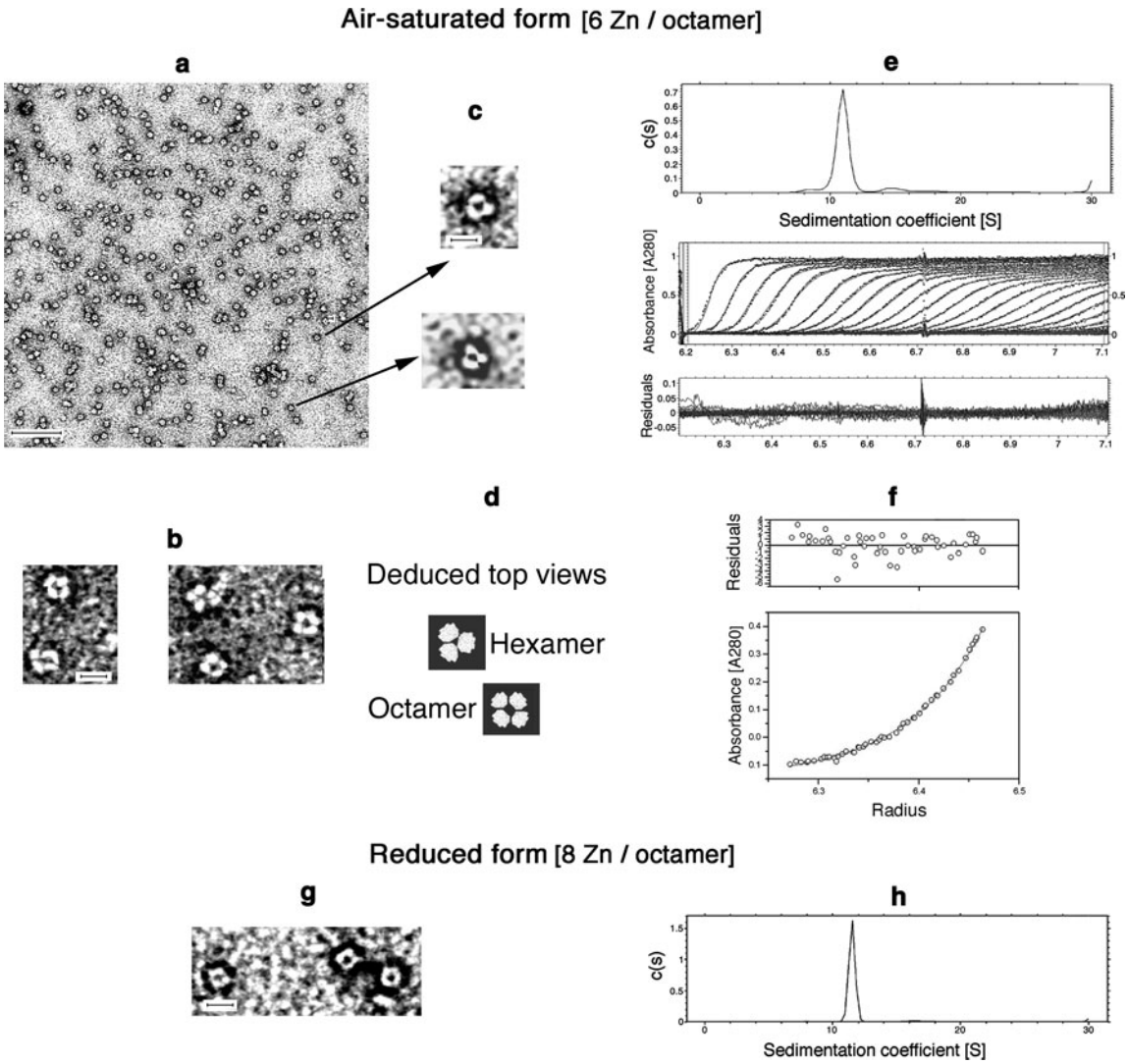

Fig. 2 Negative staining electron microscopy and analytical ultracentrifugation for PBGS under different conditions. The *top panels* (**a**, **b**, and **c**) show the PBGS oligomers under air-saturated conditions. PBGS contains six zinc ions per eight subunits. Scale bar for the panel **a** represents 100 nm. Two images (**b**) are magnified typical views (top views of four sets of a dimer-unit). *Scale bar* for the panel (**b**) represents 10 nm. Two images (**c**) are magnified typical views (top views of three sets of a dimer-unit). *Scale bar* for the panel (**c**) represents 10 nm. Two illustrates (**d**) show deduced space-filling display of the top views of an octamer and a hexamer of human PBGS (PDB code 1E51), which have been visualized using the software package RasMol. Sedimentation velocity of PBGS in a buffer under air-saturated condition (**e**); moving boundaries (*top*), residuals (*middle*), and the distribution function of sedimentation coefficients, c(s) (*bottom*). Sedimentation equilibrium of PBGS under the same conditions (**f**); residuals (*top*), and the concentration distribution in equilibrium (*bottom*). The *bottom panel* shows PBGS oligomers under reducing conditions. PBGS contains eight zinc ions per eight subunits. The *left panel* (**g**) shows a magnified typical view (a top view of four sets of a dimer-unit) under reducing conditions. *Scale bar* for the panel (**g**) represents 10 nm. Sedimentation velocity of PBGS under reducing conditions with zinc ions (**h**)

88 to 2, respectively (Table 1). In the analysis of untreated PBGS performed in 100 mM Tris buffer, pH 7.5, the ratio of octamer to hexamer was 88.3 to 3.6. In the analysis of reduced PBGS (8 zinc ions/octamer) performed in 100 mM Tris buffer, pH 7.5, the ratio of octamer to hexamer was 97 to 3.

These findings are partly consistent with the previous reports (Breinig et al. 2003; Tang et al. 2006), and the "morpheein" concept (Jaffe 2005); each oligomer is assembled by different conformational dimer-units with same primary structure, although the content of the hexamer is much lower. The present electron microscopic images of octamer and hexamer are consistent with these results, but the ratio of hexamer to octamer did not change with enzyme concentration (data not shown). At this stage, there is no strong evidence that the hexamer and octamer species are in equilibrium.

Native PAGE analysis of PBGS under air-saturated conditions shows one major band with a minor electrophoretically faster species, which is in good agreement with the results of analytical ultracentrifugation and electron

Table 1 Sedimentation velocity for PBGS (6 zinc ions/octamer) in various buffer concentrations

Buffer (mM)	Sedimentation coefficient (S)	Relative abundance[a] (%)	Estimated molecular mass based on c (M) by SEDFIT (Da)	Subunit number[b]
30	5.91	5.5	176,000	4.9 (6)
	7.65	86	259,000	7.1 (8)
50	5.84	5	183,500	5.1 (6)
	8.56	89	269,000	7.4 (8)
75	5.62	4	178,000	4.9 (6)
	7.41	87	269,000	7.4 (8)
100	5.41	2	172,000	4.7 (6)
	7.18	88	260,000	7.1 (8)
150	11.07	88	271,000	7.5 (8)

[a] The relative abundance was estimated by the area under c(s) profile

[b] Each subunit number was calculated as oligomer mass/human PBGS molecular mass (36.3 kDa). The presumed number of subunits from the experimental data are listed in parentheses. It is seen from the table that the experimentally determined numbers are generally slightly smaller than the presumed stoichiometry. This may have arisen from the conformational equilibrium of the oligomers, which could broaden the moving boundaries

microscopic analyses, where octamer is observed, as a dominant species with some minor hexamer, although somewhat different proportions are obtained depending on the methods utilized. The difference in these results has been very likely caused by the different principle of each analysis. In electron microscopy, the efficiency of adsorption to the grid may vary among molecular species. Also, it is not surprising if native PAGE, which is a zonal (band) method, and sedimentation velocity, which is a boundary method with constant concentrations at the plateau region, give different ratio of the different molecular species (Arakawa et al. 2006).

The oligomeric states of F12L on analytical ultracentrifugation (Phe^{12} is replaced with Leu) (PDB 1PV8) were revealed to be tetramer and hexamer (the ratio of tetramer to hexamer was 70 to 30) (Breinig et al. 2003), that of R240A (Arg^{240} is replaced with Ala) dimer and hexamer (almost all hexamer) (Tang et al. 2006), and that of W19A (Trp^{19} is replaced with Ala) monomer, dimer, and hexamer (almost all dimer) (Tang et al. 2006). Analysis of band density of native PAGE for oligomeric states of R240W (Arg^{240} is replaced with Trp) revealed to be octamer and hexamer (the ratio of band density for octamer to hexamer

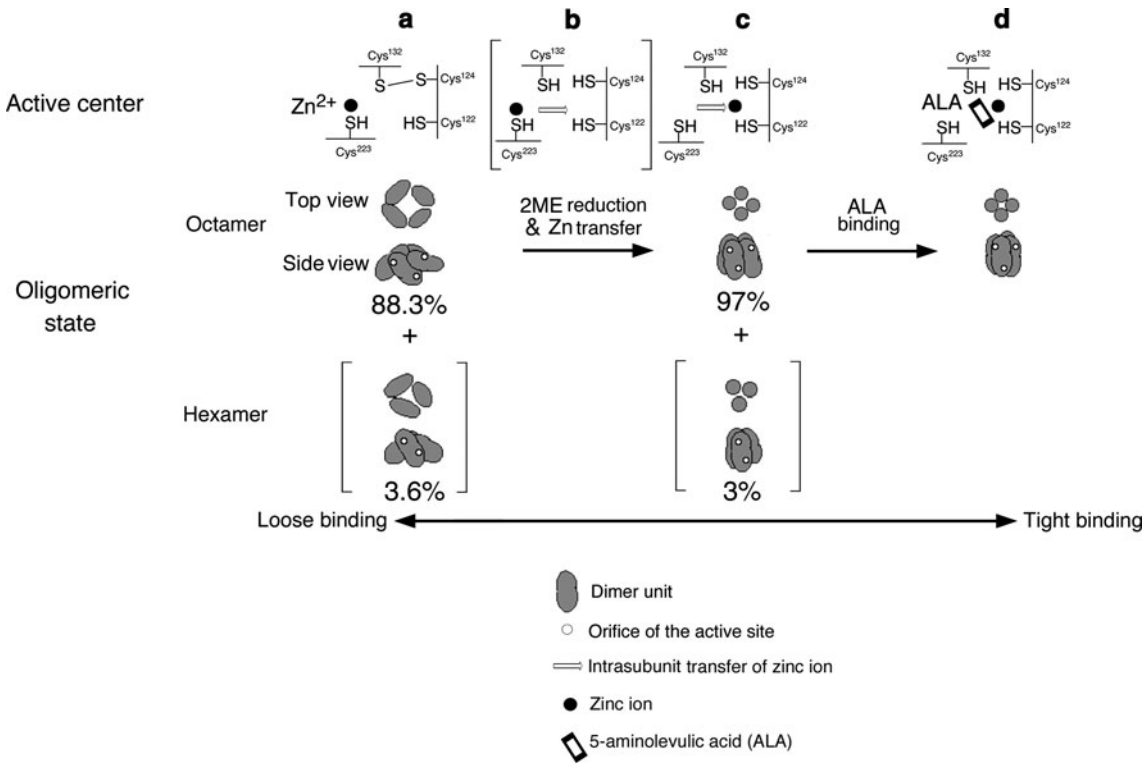

Fig. 3 Proposed change of the oligomeric state in the enzymatic activity. **a** Oligomeric state showing a relatively staggered conformation under air-saturated conditions; **b** oligomeric state during release of distal zinc ions, and intrasubunit transfer of these ions under reducing conditions (precise mechanism was explained in the previous report (Sawada et al. 2005); **c** oligomeric state of proximal zinc-bound form under reducing conditions (less staggered and more packed conformation); **d** oligomeric state of substrate ALA (5-aminolevulinic acid)-bound and fully active form. The molecular weight of octamer reduces by reduction. Details are described in Sect. "Discussion"

was 20 to 80) (Jaffe and Stith 2007). These findings suggest that Phe^{12}, Arg^{240}, and Trp^{19} are essential to stabilize the octamer of PBGS and the enzymatic activity (Breinig et al. 2003; Tang et al. 2006).

Our previous study revealed that reducing reagent induces "release of distal zinc ions, intrasubunit transfer of these ions, and binding to the proximal zinc-binding site" to fully activate PBGS (Sawada et al. 2005). Based on a hypothesis that change in oligomeric state induces PBGS activation, we studied and concluded that four sets of a dimer unit in the octamer of PBGS under air-saturated conditions form a relatively staggered conformation (Fig. 3a), but subunits in the PBGS complex were loosely bound and some dimer subunit would be released under air-saturated conditions. Further, oligomeric state of PBGS under reducing conditions toward full activation of the enzyme, became tightly packed as indicated by the frictional ratio (Fig. 3c). They were so tightly bound that a dimer unit was hardly released from an octamer under the conditions.

References

Arakawa T, Philo JS, Ejima D, Tsumoto K, Arisaka F (2006) Morpheeins—a new structural paradigm for allosteric regulation, trends. BioProcess Int 4:32–42

Bevan DR, Bodlaender P, Shemin D (1980) Mechanism of porphobilinogen synthase. Requirement of Zn^{2+} for enzyme activity. J Biol Chem 255:2030–2035

Brandt U, Kerscher S, Dröse S, Zwicker K, Zickermann V (2003) Proton pumping by NADH:ubiquinone oxidoreductase. A redox driven conformational change mechanism? FEBS Lett 545:9–17

Breinig S, Kervinen J, Stith L, Wasson AS, Airman R, Wlodawer A, Zdanov A, Jaffe EK (2003) Control of tetrapyrrole biosynthesis by alternate quaternary forms of porphobilinogen synthase. Nature Struct Biol 10:757–763

Cedervall T, Berggård T, Borek V, Thulin E, Linse S, Åkerfeldt KS (2005) Redox sensitive cysteine residues in calbindin D28 k are structurally and functionally important. Biochemistry 44:684–693

Cheh A, Neilands JB (1973) Zinc, an essential metal ion for beef liver delta aminolevulinate dehydratase. Biochem Biophys Res Commun 55:1060–1063

Erskine PT, Senior N, Awan S, Lambert R, Lewis G, Tickle IJ, Sarwar M, Spencer P, Thomas P, Warren MJ, Shoolingin-Jordan PM, Wood SP, Cooper JB (1997) X-ray structure of 5-aminolaevulinate dehydratase, a hybrid aldolase. Nat Struct Biol 12:1025–1031

Erskine PT, Coates L, Newbold R, Brindley AA, Stauffer F, Wood SP, Warren MJ, Cooper JB, Shoolingin-Jordan PM, Neier R (2001) The X-ray structure of yeast 5-aminolaevulinic acid dehydratase complexed with two diacid inhibitors. FEBS Lett 503:196–200

Frère F, Schubert WD, Stauffer F, Frankeberg N, Neier R, Jahn D, Heinz DW (2002) Structure of porphobilinogen synthase from *Pseudomonas aeruginosa* in complex with 5-fluorolevulinic acid suggests a double Schiff base mechanism. J Mol Biol 320:237–247

Jaffe EK (2005) Morpheeins—a new structural paradigm for allosteric regulation. Trends Biochem Sci 30:490–497

Jaffe EK, Stith L (2007) ALAD porphyria is a conformational disease. Am J Hum Genet 80:329–337

Jaffe EK, Salowe SP, Chen NT, DeHaven PA (1984) Porphobilinogen synthase modification with methylmethanethiosulfonate. A protocol for the investigation of metalloproteins. J Biol Chem 259:5032–5503

Jaffe EK, Martins J, Li J, Kervinen J, Dunbrack RL Jr (2001) The molecular mechanism of lead inhibition of human porphobilinogen synthase. J Biol Chem 276:1531–1537

Kervinen J, Jaffe EK, Stauffer F, Neier R, Wlodawer A, Zdanov A (2001) Mechanistic basis for suicide inactivation of porphobilinogen synthase by 4, 7-dioxosebacic acid, an inhibitor that shows dramatic species selectivity. Biochemistry 40:8227–8236

Laemmli UK (1970) Cleavage of structural proteins during the assembly of the head of bacteriophage T4. Nature 227:680–685

Li X, de Leeuw E, Lu W (2005) Total chemical synthesis of human psoriasin by native chemical ligation. Biochemistry 44:14688–14694

Mauzerall D, Granick S (1956) The occurrence and determination of delta-amino-levulinic acid and porphobilinogen in urine. J Biol Chem 219:435–446

Nagahara N, Katayama A (2005) Post-translational regulation of mercaptopyruvate sulfurtransferase via a low redox potential cysteine-sulfenate in the maintenance of redox homeostasis. J Biol Chem 280:34569–34576

Pazicni S, Cherney MM, Lukat-Rodgers GS, Oliveriusová J, Rodgers KR, Kraus JP, Burstyn JN (2005) The heme of cystathionine beta-synthase likely undergoes a thermally induced redox-mediated ligand switch. Biochemistry 44:16785–16795

Philo JS, Rosenfeld R, Arakawa T, Wen J, Narhi LO (1993) Refolding of brain-derived neurotrophic factor from guanidine hydrochloride: kinetic trapping in a collapsed form which is incompetent for dimerization. Biochemistry 32:10812–10818

Sawada N, Nagahara N, Sakai T, Nakajima Y, Minami M, Kawada T (2005) The activation mechanism of human porphobilinogen synthase by 2-mercaptoethanol: intrasubunit transfer of a reserve zinc ion and coordination with three cysteines in the active center. J Biol Inorg Chem 10:199–207

Schuck P (2000) Size-distribution analysis of macromolecules by sedimentation velocity ultracentrifugation and Lamm equation modeling. Biophys J 78:1606–1619

Sevrioukova IF (2005) Redox-dependent structural reorganization in putidaredoxin, a vertebrate-type [2Fe-2S] ferredoxin from *Pseudomonas putida*. J Mol Bol 347:607–621

Shoolingin-Jordan PM, Spencer P, Sarwar M, Erskine PE, Cheung KM, Cooper JB, Norton EB (2002) 5-Aminolaevulinic acid dehydratase: metals, mutants and mechanism. Biochem Soc Trans 30:584–590

Tang L, Breinig S, Stith L, Mischel A, Tannir J, Kokona B, Fairman R, Jaffe EK (2006) Single amino acid mutations alter the distribution of human porphobilinogen synthase quaternary structure isoforms (morpheeins). J Biol Chem 28:6682–6690

Zirah S, Kozin SA, Mazur A, Blond A, Cheminant M, Ségalas-Milazzo I, Debey P, Rebuffat S (2006) Structural changes of region 1–16 of the Alzheimer disease amyloid beta-peptide upon zinc binding and in vitro aging. J Biol Chem 281:2151–2161